The vertical capacity of grillage foundations

Bransby, M.F.; Knappett, J.A.; Brown, M.J.; Hudacsek, P.

Published in:
Géotechnique

DOI:
10.1680/geot.9.P.131

Publication date:
2012

Document Version
Publisher's PDF, also known as Version of record

Bransby, M. F. *et al.* (2012). *Géotechnique* **62**, No. 3, 201–211 [http://dx.doi.org/10.1680/geot.9.P.131]

The vertical capacity of grillage foundations

M. F. BRANSBY*, J. A. KNAPPETT†, M. J. BROWN† and P. HUDACSEK†

Grillage foundations may provide an economical alternative to offshore 'mudmat' foundations for seabed infrastructure, owing to their improved hydrodynamic characteristics, which are important during installation. Grillage foundations consist of a mesh of vertical grilles that penetrate the seabed during loading. Offshore loadings on these types of foundation are likely to consist of vertical (mostly dead weight) loading and horizontal 'in-service' loads. However, to date there is no accepted method of design, as foundation capacity may differ significantly from that of conventional solid shallow foundations. This paper presents an analytical method designed to calculate the variation of vertical bearing capacity with grille penetration in sand. The results show that grillages are able to achieve the same capacity as solid foundations of the same breadth, but this requires significant penetration of the grillage. Consequently, design choices are likely to depend on the amount of settlement the structure can tolerate. Simplified analytical equations have been presented to allow calculation of the load–settlement response, and to calculate how much settlement is required to mobilise the flat-plate capacity of a solid mudmat of the same overall breadth. The methodology has been validated by comparing results with those from model tests.

KEYWORDS: bearing capacity; footings/foundations; model tests; offshore engineering; sands

Les fondations à grillage pourraient offrir une alternative économique aux fondations à radier en mer pour des infrastructures sur fond marin, en raison de leurs propriétés hydrodynamiques supérieures, qui sont importantes au cours de l'installation. Les fondations à grillage comportent un treillis de grilles verticales pénétrant dans le fond matin au cours de la charge. Les charges en mer de ces type de fondations se composent probablement de charges verticales (à poids mort) et horizontales « en service ». Toutefois, jusqu'à présent, aucune méthode d'étude reconnue n'a été établie, car la capacité des fondations pourrait être sensiblement différente de celle des fondations pleines traditionnelles de faible profondeur. Cette communication présente une méthode analytique conçue pour calculer la variation de la force portante en fonction de la pénétration de la grille dans le sable. Les résultats montrent que les grillages permettent de réaliser la même force portante que des fondations pleines de même largeur, à condition d'assurer une pénétration significative du grillage. En conséquence, les choix de principe dépendront probablement du degré de tassement que la structure pourra tolérer. Des équations analytique simplifiées sont présentées pour permettre le calcul de la réaction charge /tassement, et du degré de tassement nécessaire pour mobiliser la force de dalle plate d'un radier plein de la même largeur globale. On a validé cette méthodologie en comparant les résultats avec des résultats obtenus sur maquette.

INTRODUCTION

Offshore infrastructure such as pipeline end manifolds (PLEM), pipeline end terminations (PLET) and temporary anchors may be supported by shallow foundations. In such cases the foundations can consist of a single large foundation ('mudmat') or sometimes multiple foundations supporting the same structure (Fisher & Cathie, 2003). Shallow foundations can either rest on the surface, or may be skirted if large loadings are expected.

When seabed infrastructure is placed on the seabed it is initially subjected to the vertical dead weight structural loading, W. During operation, additional loadings are likely to be horizontal, H, as a result of (a) pipeline expansion or jumper loads, (b) snag loads (from trawling or anchoring), or (c) hydrodynamic loads (in shallow water). In most cases these will be applied relatively close to the level of the seabed (because the manifold structures are relatively flat compared with their breadth), so that moment loads, M, are normally small. Hence it is the combinations of vertical dead weight and the additional horizontal load that govern the choice of foundation type and size.

Pipeline structures are placed on the seabed by lowering them from a vessel. If the structure is relatively large, this operation can be conducted only in good sea conditions, because otherwise lowering the structure through the splash zone is hazardous. This means that installation may require additional expensive vessel time waiting for appropriate weather conditions.

A grillage foundation is an attractive alternative to a conventional mudmat foundation, reducing dead weight and hydrodynamic loading in the splash zone. Grillage foundations (Figs 1 and 2) consist of multiple thin vertical grilles connected rigidly together to form the foundation. Typically, the grille thickness $t = 5–10$ mm, the grille height $D = 50$ mm, and the centre-to-centre spacing s may vary from 20 mm to 80 mm depending on the design. These foundations have the advantage that water can move freely between the grilles, and so a structure may be lowered easily through the splash zone, even in poor sea states. Clearly, this will have financial advantages to the contractor, as it is likely to reduce offshore installation times. In addition, there is a possibility that the foundations may require less steel than conventional mudmat foundations.

To date, grillage foundations have been used in several offshore projects. However, as yet there is no generally accepted method to calculate their bearing capacity under either pure vertical or combined vertical–horizontal loading. In addition, it is uncertain how bearing capacity is affected by the spacing s of the grilles and their thickness t (or most likely the spacing ratio, s/t) for different soil conditions. It remains to be found for what soil conditions and spacing ratios are the bearing capacity and combined load capacity

Manuscript received 4 November 2009; revised manuscript accepted 12 April 2011. Published online ahead of print 25 November 2011. Discussion on this paper closes on 1 August 2012, for further details see p. ii.

* Advanced Geomechanics, Australia (formerly University of Dundee, UK).
† University of Dundee, UK.

Fig. 1. Typical subsea frame (3 m × 4 m plan area) with grillage foundation. Image courtesy of Subsea 7, UK

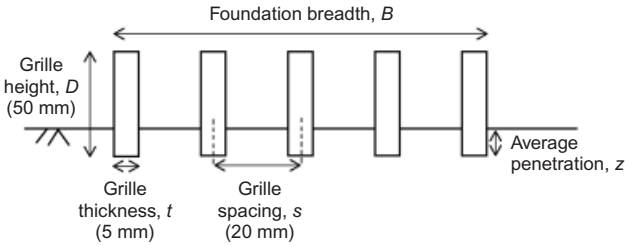

Fig. 2. Grillage geometry (not to scale; typical dimensions in brackets)

of grillage foundations sufficient such that they can be used as alternative foundations.

To address this, a joint industry project (Acergy, Subsea 7, Technip, Cathie Associates and University of Dundee) was conducted with the aims of: (a) understanding how grillage foundations interact with the seabed; and (b) producing a method for their design. As part of this project, a series of laboratory physical model tests was conducted by the University of Dundee. These tests investigated the vertical bearing capacity of grillage foundations and the combined vertical (V) – horizontal (H) capacity in drained, sandy soil. This paper concentrates on the vertical capacity of grillage foundations.

The geometry of grillage foundations is shown schematically in Fig. 2. Note that the number of grilles is shown as $N = 5$ in the figure, but this will be significantly larger in a real foundation system. When vertical load V is applied, the foundation will penetrate vertically into the soil by an amount z, which may be several times the grille thickness t. It is the relationship between the vertical penetration and the applied vertical load (for a given grillage geometry) that is required for design.

A rigid connection system connects each grille at the connection to the superstructure so that each individual grille is prevented from rotating or displacing laterally or vertically compared with its neighbours. Consequently, the individual grilles have some similarity with the interfering shallow foundations studied by previous researchers (Stuart, 1962; Graham *et al.*, 1984; Javadi & Spoor, 2004; Kumar & Ghosh, 2007). However, these previous studies investigated foundations with negligible embedment, and so the findings may be less relevant to grillages as foundation penetration increases. It will be shown later that, for larger penetrations, the soil between each pair of grilles may be considered to act more like a plugged pile, and so previous findings from research on plugged piles (Randolph *et al.*, 1991) may be applied to the problem.

TESTING APPARATUS AND METHODOLOGY

Foundation properties

Grillage foundations were constructed from multiple, smooth steel plates each of thickness, $t = 5$ mm or 10 mm, length $L = 300$ mm (to give plane-strain conditions), and height $D = 150$ mm (Fig. 2). They were connected together with six bars and spacer blocks for rigidity, and to ensure that each grille was parallel (Fig. 3). This system allowed both the spacing s between the grilles and the number of grilles N to be varied between tests.

A full-scale grillage foundation would have many grilles, N (a 3 × 4 m seabed frame is shown in Fig. 1). A typical 3 m wide foundation with $s = 30$ mm would have $N = 3000/30 = 100$. The aim of the tests conducted here was to capture the detailed soil–grille interaction, and so full-scale grilles were tested, thus making testing of a large number of grilles unfeasible under laboratory conditions. Grillages with $N = 2$, 5 and 8 were tested to examine the influence of the number of grille units on the resulting soil–grillage interaction. The alternative approach of testing large numbers of grilles at reduced scale might have introduced significant stress-level or grain-size scaling effects. The influence of N on the grillage–soil interaction will be discussed later in the paper.

In addition, only plane-strain loading conditions have been investigated in the tests. However, grilles are likely to be

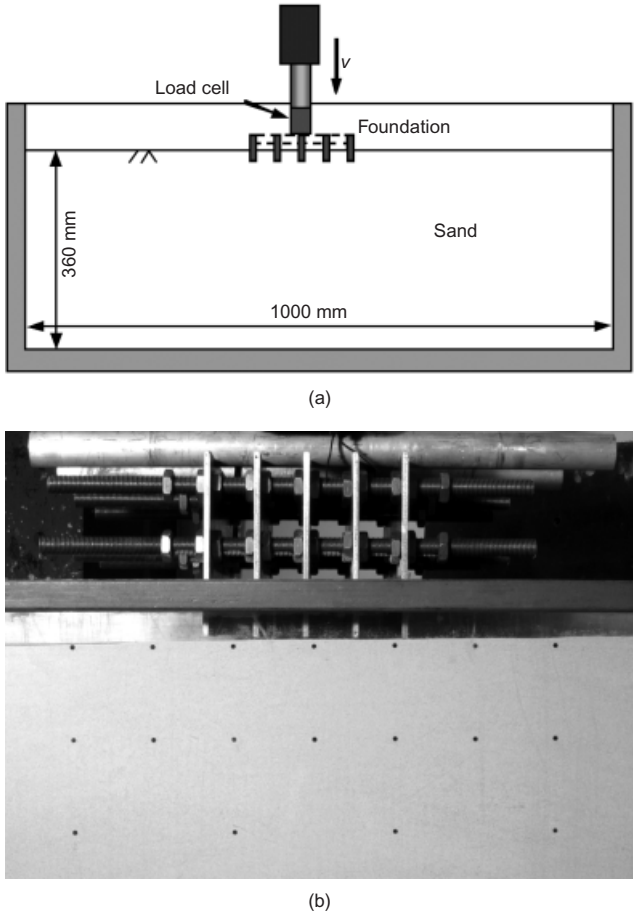

Fig. 3. Vertical grillage testing apparatus: (a) schematic diagram of apparatus; (b) photograph of grillage foundation ($N = 5$, $t = 5$ mm, $s/t = 8$)

orientated parallel to each other with a small number of cross-grilles to ensure stability, and so the test conditions investigated may be appropriate.

Soil beds

Dry soil beds were contained in a box 1000 mm long and 300 mm broad, which was filled to a depth of 360 mm (Fig. 3(a)). The front face of the box was constructed from Perspex to allow the deformation of the soil and foundation to be photographed. Image analysis (described later) was then used to extract information about soil displacements from these images. Dry sand was used to ensure that drained soil conditions were achieved during loading.

The soil used was a uniform fine silica sand with $d_{50} = 0{\cdot}18$ mm, $d_{10} = 0{\cdot}12$ mm, $\rho_{max} = 1760$ kg/m^3 and $\rho_{min} = 1461$ kg/m^3. During the experimental programme, loose, medium and dense soil beds were prepared, but this paper will focus on tests conducted in loose sand. These ground conditions represent those that are likely to give the lowest capacity, and which are therefore those in which accurate assessment of grillage capacity will be most critical. To prepare the loose beds, an open-weave mesh (3 mm diameter holes, 33% open area) of similar dimensions to the box was placed at the base of the box. Sand was then placed in the box, and the base mesh was slowly extracted through the soil. During extraction of the mesh, the soil sheared to critical state, giving a loose condition. The density of the soil was measured and found to be uniform with $\rho = 1487$ kg/m^3 (relative density $D_r \approx 9\%$).

Soil properties

Direct shear box tests were undertaken using a standard 60 mm square shear box to BS 1377 (BSI, 1990) on dry sand/sand samples. Similar testing was undertaken for the sand/steel interface, in which the lower half of the shear box was replaced by a solid steel block of similar surface roughness to the grillage plates. In both series of tests the sand was prepared at relative densities designed to mimic those used during the model grillage testing. Sand samples were sheared at a constant rate of 1·2 mm/min.

Table 1 shows a summary of the failure envelope parameters determined from the shear box tests for loose soil for both soil/soil shear and soil/steel interface tests. Results are shown for best fits to the peak shear stress against normal stress data, and also where the best-fit line has been forced through the origin ($c' = 0$). Tests were undertaken at normal stresses of 10, 20 50, 100 and 200 kPa, to ensure that the failure envelopes applied equally well in the low- and high-stress ranges.

Methodology and test programme

The apparatus for vertical loading is shown in Figs 3(a) and 3(b). The grillage foundation was attached to a 300 mm stroke hydraulic actuator by way of a tension–compression load cell. A linearly variable differential transformer (LVDT) was placed behind the actuator on the foundation centreline to measure the vertical position of the foundation. The actuator displaced the foundation vertically downwards at a velocity of approximately 0·4 mm/s. Digital photographs were captured of the front face of the container corresponding to a displacement increment of approximately 6 mm. Each test was stopped just before the connections between the grilles came into contact with the soil, which typically required approximately 60 mm of displacement.

Table 2 summarises the tests that are used to validate the analytical model developed herein. Most of the grillages discussed herein have $N = 5$ grille elements. In addition to the grillage geometries tested, Table 2 also shows the equivalent capacity of a solid flat plate of equivalent breadth B, $V_{0,flatplate}$, calculated following DNV (1992) for a surface-bearing foundation ($z = 0$). This represents the equivalent mudmat that the grillage would be expected to replace. Where this capacity has been exceeded during the load test, the vertical displacement required to mobilise $V_{0,flatplate}$ is recorded in Table 2 (z_0). The maximum possible vertical capacity V that can be provided by the grillage (i.e. at its maximum penetration of $z = 50$ mm) is also given, normalised by $V_{0,flatplate}$.

Typical load–penetration curves for grillages at various s/t and t (but all with $N = 5$) are shown in Fig. 4.

ANALYTICAL SOLUTIONS

Three different analytical calculation methods will be used to predict grillage foundation bearing capacity, depending on the mechanism of load transfer. These are discussed in turn below.

Flat plate (fully plugged) analysis

For the solid foundation (or fully plugged) assumption it is assumed that the soil between the grilles moves as part of the foundation. Hence the foundation system behaves as an equivalent flat plate of breadth B (defined by the external dimensions of the grilles; Fig. 2) and penetration depth z. The DNV (1992) bearing capacity calculation method is used to calculate the bearing pressure at failure, q_f.

$$q_f = 0{\cdot}5\gamma' B N_\gamma d_\gamma + \left(\gamma' z + \frac{c'}{\tan\phi'}\right) N_q d_q \qquad (1)$$

where $q_f = V/A$; the base area $A = BL$; γ' is the effective unit weight of the soil; c' is the apparent cohesion; N_γ and N_q are bearing capacity factors that vary with the angle of

Table 1. Summary of failure envelope parameters determined for loose sand in direct shear box tests

Property	Soil/soil	Soil/steel interface
ϕ'_{peak}, $c' = 0$: degrees	30·8	–
ϕ'_{peak}: degrees	30·5	–
c': kPa	1·0	–
δ'_{peak}, $c' = 0$: degrees	–	21·7
δ'_{peak}: degrees	–	20·6
c': kPa	–	3·1

Table 2. Vertical bearing capacity (V_0) tests

Test ID	t: mm	s/t	N	$V_{0,flatplate}$:* kN	z_0: mm	$V/V_{0,flatplate}$ at $z = 50$ mm: %
V4	5	4	2	0·028	7·7	747
V5	5	4	5	0·325	23·7	203
V6	5	4	8	0·946	36·6	153
V10	5	8	2	0·091	34·0	153
V11	5	8	5	1·225	–	34·3
V12	5	8	8	3·654	–	23·7
V16	5	2·5	5	0·136	10·3	408
V18	5	6	5	0·703	–	74·8
V22	10	8	5	4·899	–	13·3
V23	10	4	5	1·300	–	74·2

* Calculated using equation (1) with $z = 0$.

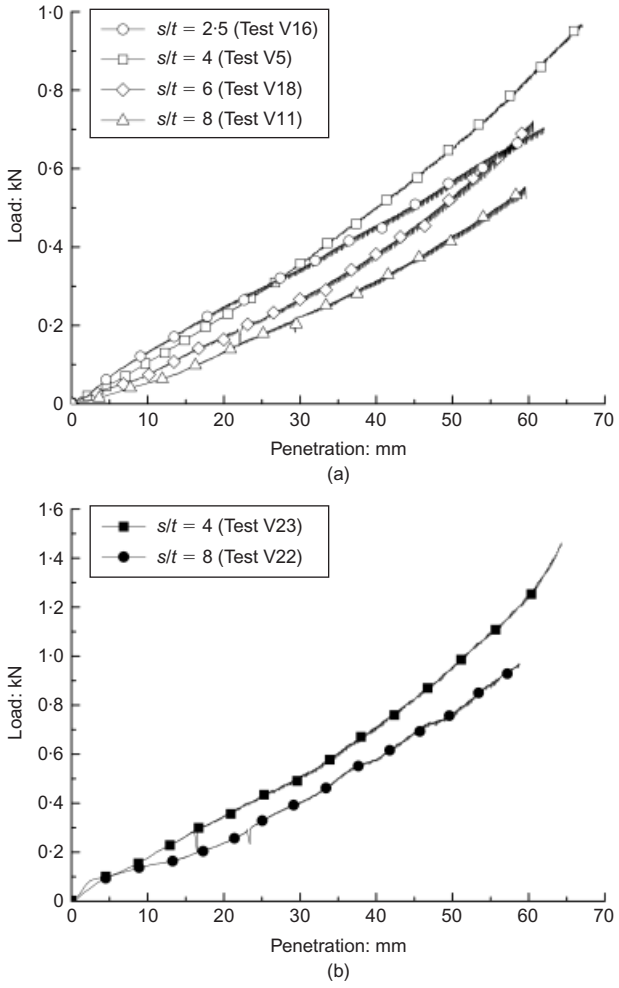

Fig. 4. Load–penetration test data for grillage foundations with $N = 5$ in loose sand: (a) $t = 5$ mm; (b) $t = 10$ mm

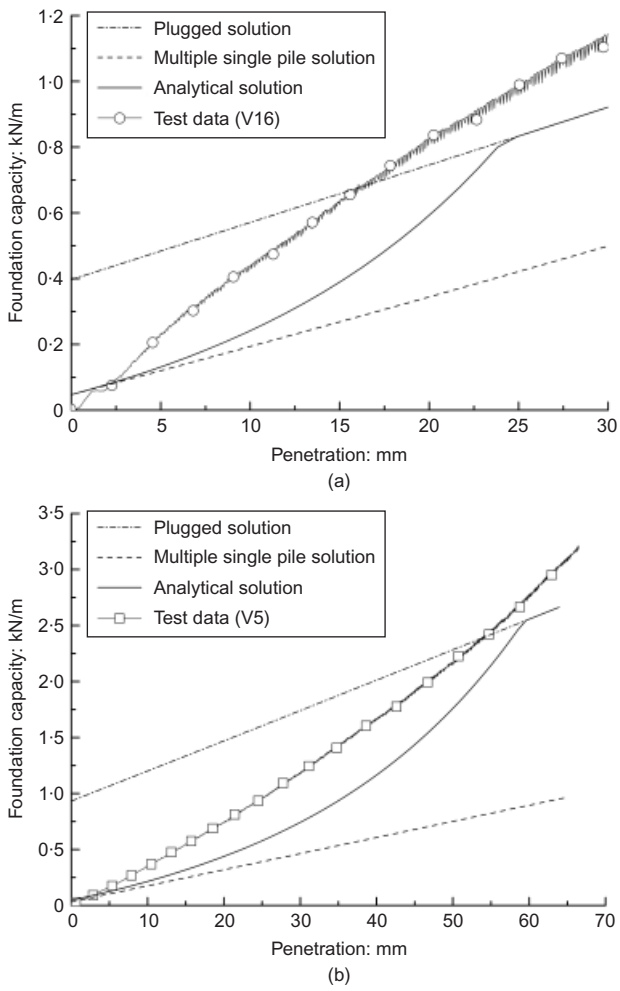

Fig. 5. Comparison of analytical solutions with load test data: (a) $s/t = 2{\cdot}5$; (b) $s/t = 4$ ($\phi = 30{\cdot}8°$; $\delta = 21{\cdot}7°$; $\gamma = 14{\cdot}59$ kN/m^3; $K = 1{\cdot}5K_0$)

friction ϕ' of the soil; and d_q and d_γ are depth correction factors. Reissner (1924) found the closed-form solution for N_q appropriate to shallow foundations, as

$$N_{q\mathrm{R}} = \mathrm{e}^{\pi \tan \phi} \tan^2 \left(45 + \frac{\phi'}{2}\right) \tag{2}$$

with the additional subscript 'R' used in $N_{q\mathrm{R}}$ to denote the Reissner (1924) shallow foundation solution. Hansen (1970) suggested empirically that

$$N_\gamma = 1{\cdot}5(N_q - 1)\tan \phi' \tag{3}$$

DNV (1992) recommends that $d_q = 1$, and the depth correction factor for overburden is given as

$$d_\gamma = 1 + 1{\cdot}2\frac{z}{B}\tan \phi'(1 - \sin \phi')^2 \tag{4}$$

Figure 5 shows calculated foundation capacity (plugged solution) against grille penetration z for two foundations with $t = 5$ mm, $s/t = 2{\cdot}5$ and 4, and $N = 5$ in loose sand. The properties of the sand used in all the calculations reported in this paper were selected to match those of the experimental programme, namely $\rho = 1487$ kg/m^3 with the shear strength properties given in Table 1. Allowance was also made for lateral friction on the outside of the external grilles. There is a significant capacity at zero penetration/embedment (associated with the first term of equation (1)) and then increasing capacity with further foundation penetration. The loads measured in the model tests start at zero and increase with penetration, eventually reaching the capacity of the equivalent embedded flat plate (plugged solution) at $z = 15$ mm and 55 mm for $s/t = 2{\cdot}5$ and 4 respectively. The plugged solution is therefore not appropriate for modelling the grillage capacity at low penetration.

Multiple pile calculations (no interaction)

This solution assumes that each grille acts as a single, plane-strain pile where each is unaffected by the others around it. Therefore the capacity of each grille is obtained by summing the base resistance and the skin friction as for axially loaded piles, which is multiplied by N to give the overall foundation capacity.

The base capacity Q_b of each grille is given by a slightly modified version of the standard pile end-bearing equation to allow for the base area of each grille ($A_\mathrm{b} = tL$).

$$Q_\mathrm{b} = tL\sigma'_{\mathrm{vb}}N_{q\mathrm{B}} + 0{\cdot}5\gamma' N_\gamma t^2 L \tag{5}$$

where the vertical effective stress at the level of the grille tips, $\sigma'_{\mathrm{vb}} = \gamma' z$. As in conventional pile design, the second term of equation (5) is much smaller than the first term as soon as grille penetrations become significant compared with the grille thickness. $N_{q\mathrm{B}}$ for this case is taken from Berezantzev *et al.* (1961).

For a uniform soil layer, the skin friction on each side of a grille of length L and penetration depth z is

$$Q_\mathrm{s} = (0{\cdot}5K\gamma' z \tan \delta')zL \tag{6}$$

where K is the lateral earth pressure coefficient and δ' is the interface friction angle between the soil and the grille. K is taken to be $1{\cdot}5K_0$ based on the recommendations of Kulhawy (1984) for large-displacement piles, with K_0 determined using Jaky's (1944) equation. The overall capacity of the foundation is thus

$$V = N(Q_b + 2Q_s) \tag{7}$$

This is plotted in Fig. 5 for $K = 0{\cdot}73$ and $\delta' = 21{\cdot}7°$ (as measured in the interface tests). These values of K and δ' were used in all subsequent calculations reported in this paper.

Figure 5 suggests that the isolated pile calculations give foundation capacities that increase with embedment depth, but never exceed the plugged foundation capacity. This suggests that the soil will fail by the grillage units penetrating into the soil ('coring'), and the soil will never plug: the foundation capacity–penetration relationship is predicted to follow the multiple single pile line in Fig. 5. The load–penetration curve from the model test data can be seen initially to follow this line at low penetration, but it soon diverges towards the plugged solution described in the previous section.

Multiple pile calculations with silo/arching effect

The foregoing analysis ignores the fact that the closely spaced grilles will increase the vertical (and therefore horizontal) stress between them, as observed for plugging pipe piles (Randolph *et al.*, 1991).

Consider the soil between two adjacent grilles. Fig. 6 shows the forces acting on a block of thickness dz between grilles, where z is the depth below the ground surface. Uniform vertical stress conditions are assumed to act along the base and top of the soil element (a conservative assumption for both Q_s and Q_b), and so by examining the vertical equilibrium of the soil element

$$\frac{d\sigma'_v}{dz} = \gamma' + \frac{2\tau}{s-t} \tag{8}$$

Given that

$$\tau = K\sigma'_v \tan\delta' \tag{9}$$

equations (8) and (9) can be combined to give

$$\frac{d\sigma'_v}{dz} = \gamma' + \frac{2K\tan\delta'}{s-t}\sigma'_v \tag{10}$$

Equation (10) can be rearranged to find the distribution of vertical stress with depth.

$$\int_0^{\sigma_v} \frac{d\sigma'_v}{\gamma' + \left(\dfrac{2K\tan\delta'}{s-t}\right)\sigma'_v} = \int_0^z dz \tag{11}$$

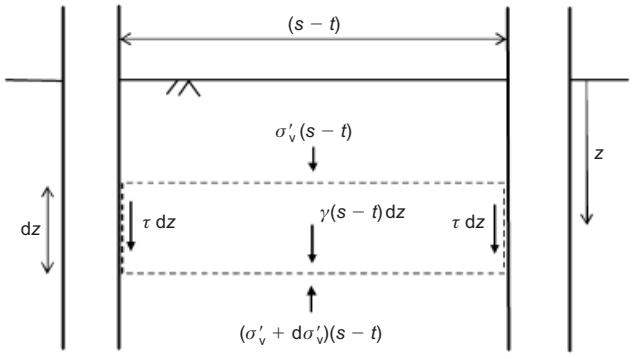

Fig. 6. Forces (per m length) acting on a soil block between grilles

$$\sigma'_v = (e^{az} - 1)\frac{\gamma'}{a} \tag{12}$$

where $a = 2K\tan\delta'/(s-t)$, which is similar to the solution of Randolph *et al.* (1991) for pipe piles.

Figure 7 shows a typical calculated variation of vertical effective stress between grilles with depth. It is clear that the arching analysis predicts a significantly enhanced vertical effective stress compared with the free-field condition, and that this enhancement increases non-linearly with depth.

For multiple grille units the increased stress with depth will affect both the skin friction due to the enhanced normal effective stress between grilles and the end bearing of the internal grille units because of the increased overburden term (σ'_{vb}) term in equation (5).

Figure 8 shows the various soil resistance forces acting on the grillage foundation when it is penetrated vertically into soil. The total capacity of the foundation, V, is given by

$$V = 2(N-1)Q_{si} + 2Q_{so} + (N-2)Q_{bi} + 2Q_{bo} \tag{13}$$

where Q_{si} is the skin friction force on one side of each internal grille; Q_{so} is the skin friction on each of the two outside grille surfaces (assumed to be unaffected by silo action; equation (6)); Q_{bi} is the base resistance of each grille in the inside of the group; and Q_{bo} is the base resistance of each of the two external (edge) grilles. Q_{si} is found by combining equations (9) and (12) and integrating the resulting equation over the instantaneous grille length within the soil, z, to give

$$Q_{si} = \frac{\gamma' L(s-t)}{2a}(e^{az} - az - 1) \tag{14}$$

Thus it is assumed that skin friction is enhanced within each 'plug/silo' as a result of the arching effect. It is further assumed that the angle of interface friction δ' and lateral

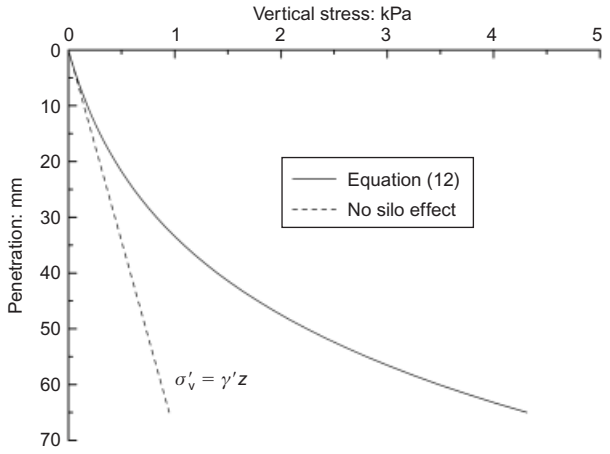

Fig. 7. Profile of calculated average vertical effective stress within grille walls ($s = 20$ mm; loose sand)

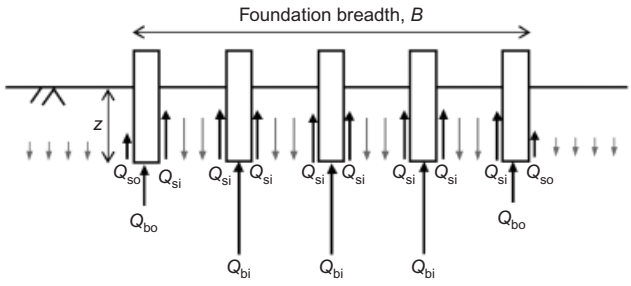

Fig. 8. Schematic diagram of soil resistance on penetrating grilles

earth pressure coefficient K are unaffected by the plug behaviour.

The base resistance of the internal grilles is assumed to be affected by the arching between the grilles. For the internal $N-2$ grilles, the N_q term of equation (5) will use the silo overburden at the grille tip depth (equation (12)). It is assumed that the N_γ and N_q values are unaffected by the other grilles.

The two edge grilles have an increased silo pressure on the internal side of the tip, and an unenhanced (i.e. $\sigma'_{vb} = \gamma' z$) stress on the external side. It is assumed that failure will be generated towards the outside (to act against the lower overburden stress), and so the end bearing resistance is calculated using $\sigma'_{vb} = \gamma' z$ in equation (5). Clearly, forcing the failure mechanism to one side is expected to generate a less efficient mechanism, and so consequently will provoke some increase in the bearing capacity factor N_q. This increase has not been considered here. However, for grillage foundations with $N \gg 2$ modification of this term will have a minimal effect on V, as the contribution from the edge grilles is outweighed by that of the internal grilles.

The results of the above analyses are shown in Fig. 5(a) for $s/t = 2{\cdot}5$ and in Fig. 5(b) for $s/t = 4$, for loose sand conditions. Equation (13) produces a non-linear increase of foundation capacity with increasing penetration depth, and the calculated capacity becomes larger than the fully plugged solution (i.e. equation (1)) at $z \approx 25$ mm for $s/t = 2{\cdot}5$ and $z \approx 60$ mm for $s/t = 4$. This suggests that when z is greater than these values, the flat plate embedded mechanism is preferable, and the soil between the grilles starts to move together with the grilles – the grilles are 'plugged'.

Comparing the analytical solution with the test data, it can be seen in both cases that the analytical solution underpredicts the measured capacity of the grillages. A change in gradient of the test data for $s/t = 2{\cdot}5$ is apparent at $z \approx$ 20 mm, which is in reasonable agreement with the predicted plugging penetration. This change in gradient is also evident in Fig. 4(a), where the capacity for a given penetration initially increases with reducing s/t until plugging occurs. Plugging is not immediately apparent from the test data for $s/t = 4$ (Fig. 5(b)), as there is no identifiable change in gradient by the end of the test. This is also evident in Fig. 4(a), where capacity increases with reducing s/t over the full penetration depth. The analytical solution suggests that the onset of plugging behaviour is imminent (Fig. 5(b)). For $s/t > 4$, plugging was not observed in the tests, or predicted using equation (13) over the depth of penetration. These observations from the load–penetration curves will be further verified by particle image velocimetry (PIV) observations later in the paper.

RESULTS FROM ANALYTICAL SOLUTIONS

The calculation methods above are used to predict three particular characteristics of grillage foundations: (a) the vertical load–displacement relationship; (b) the vertical penetration required to reach plugging conditions; and (c) the vertical penetration required to generate the design capacity of a flat-plate foundation of the same breadth. This predicted behaviour will be compared with the test data presented in Table 2.

Prediction of load–penetration curves

Figure 9 shows how foundation bearing pressure q ($= V/BL$), which is also the foundation capacity under subsequent vertical loading, increases with penetration z. Calculations were performed for loose sand conditions (see Table 1), and for

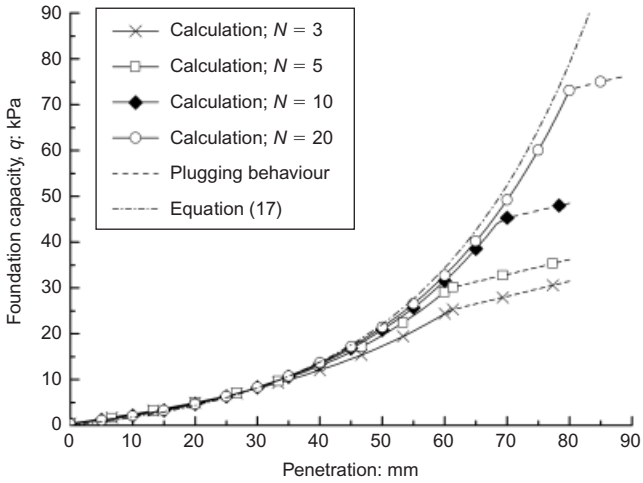

Fig. 9. Calculation of foundation capacity–penetration relationship (loose sand; $s/t = 4$; $t = 5$ mm)

$t = 5$ mm and $s/t = 4$. Initially, the multiple arching pile solution governs the curve, and the foundation capacity increases non-linearly with penetration because of equation (12). At higher penetrations the flat-plate solution (equation (1)) gives the lower foundation capacity, and so plugging is inferred and the foundation capacity increases more slowly with further penetration.

Plugged conditions are denoted by dotted lines (change in line type) in Fig. 9. The plugging pressure increases with the number of grilles, because the flat plate capacity increases with foundation breadth (and $B = (N-1)s + t$) because of equation (1). There is a consequent increase in the displacement required to plug the foundation with N due to this effect. This will be discussed further in the next section.

Before plugging occurs, the foundation capacity is governed by equation (13). When there are many grillage units (i.e. $N \gg 1$), as will be the case for an offshore foundation, the results follow approximately a single line before plugging. This line can be approximated by the following analysis. First, when $N \gg 1$, the Q_{so} and Q_{bo} terms become negligible because there are few (i.e. two) outside grilles compared with $N-2$ inside ones, and Q_{bo} and Q_{so} are much smaller than Q_{bi} and Q_{si} because of the silo effect. The Q_{bo} and Q_{so} terms in equation (13) can therefore be neglected. Second, for any significant penetration, the Q_{si} term is negligible compared with the Q_{bi} term, as discussed earlier. As a consequence of the above assumptions, equation (13) simplifies to give the vertical capacity $V \approx NQ_{bi}$ (for $N \gg 2$). Finally, the base pile resistance term, Q_{bi}, is given by equation (5) (with σ'_v given by equation (12)), and the second term of equation (5) is less than 10 times smaller than the first by $z/t > 2$. Consequently, the second term in equation (5) is also neglected. As a result, the load penetration curve can be simplified to

$$V = NtL(e^{az} - 1)\frac{\gamma'}{a} N_{qB} \tag{15}$$

or

$$q = \frac{V}{BL} = \frac{Nt}{B}(e^{az} - 1)\frac{\gamma'}{a} N_{qB} \tag{16}$$

The breadth of a grillage foundation, $B = (N-1)s + t$. For large values of N this may be approximated as $B \approx Ns$, and so equation (16) simplifies further to

$$q = N_{qB}\frac{t}{s}(e^{az} - 1)\frac{\gamma'}{a} \tag{17}$$

where $a = 2K\tan\delta'/(s-t)$ as before. Equation (17) is shown plotted in Fig. 9 and closely approximates the q–z relationship for foundations with large numbers of grillage units.

Equation (17) can be rearranged to express penetration depth for a given bearing pressure as

$$z = \frac{1}{a}\ln\left[1 + \frac{aq(s/t)}{\gamma' N_{q\mathrm{B}}}\right] \tag{18}$$

Equation (18) can be used to predict grillage foundation penetration if plugging does not occur and if N is large.

Prediction of penetration required for plugging

The plugging penetration is important, because after this depth the foundation has the same capacity as a solid foundation of the same overall breadth B at the same penetration. However, the foundation will generate this capacity only after a significant penetration (the plugging penetration, z_{plug}), and this may be too large for serviceability requirements. The following analyses were conducted to calculate z_{plug} for various soil and grillage conditions.

In the first method, equation (13) was used to evaluate the unplugged capacity of the foundation for a range of different embedment depths numerically. The flat-plate capacity (equation (1)) was then evaluated for a range of embedment depths and compared with the arching pile solution. The plugging depth z_{plug} was determined from the depth where the flat-plate capacity equalled that from the pile solution.

The second method was to generate a simplified equation that was then solved (as for the q–z term above) to find the depth z_{plug} when the multiple pile capacity equalled the flat plate solution. As above, it was assumed that $Q_{\mathrm{s}} \ll Q_{\mathrm{b}}$, and so Q_{s} was set to zero. The capacities of the external grilles were considered to be negligible (for large N), and so the capacity of the group was approximated as NQ_{bi}. Finally, as before, the end bearing resistance term was simplified to include only the σ'_{vb} term. Thus equation (15) was equated to the flat-plate capacity solution (equation (1)) multiplied by area to give

$$N\sigma'_{\mathrm{v}} t N_{q\mathrm{B}} = N_{q\mathrm{R}}\gamma' z_{\mathrm{plug}} B + 0{\cdot}5 N_\gamma \gamma' B^2 \tag{19}$$

By substituting equation (12), equation (19) becomes

$$\mathrm{e}^{az_{\mathrm{plug}}} - \frac{aB}{tN}\left(\frac{N_{q\mathrm{R}}}{N_{q\mathrm{B}}}\right) z_{\mathrm{plug}} = 0{\cdot}5\frac{aB^2}{tN}\frac{N_\gamma}{N_{q\mathrm{B}}} + 1 \tag{20}$$

Equation (20) can then be solved to find the plugging depth z_{plug} for any conditions.

Figure 10 shows the plugging depth calculated by the two methods for different numbers of grilles for $t = 5$ mm and $s/t = 4$ in loose sand conditions. As the number of grillage units increases, the difference between the solution from equation (20) and that from completing the full calculations reduces, because the edge grille effects become insignificant. For $N > 20$ the difference is smaller than 5%, and so this may be considered suitably accurate to reflect the foundation performance for likely foundation breadths. It should be noted that the difference between solutions does not quite converge to 0%, because the neglected term Q_{s} in equation (20) becomes more important as penetration depth increases. Note that a 1 m wide foundation with the above spacing and grille thickness would have approximately 50 grille units (50·75) and is predicted to require a penetration of 97 mm to generate full plugging conditions in loose sand.

Figure 11(a) shows plugging depth varying with spacing ratio s/t for various different-size foundations ($N = 5$, 20, 50). Plotted in the figure are both the results of equation (20) and the results of performing the full numerical calculations. For $N \geqslant 20$ the full calculation method and equation (20) are in excellent agreement for all spacing ratios ($2 \leqslant s/t \leqslant 8$), emphasising the likely applicability of equation (20) for foundations with many grille units. Fig. 11(a) shows that whatever the number of grilles, the plugging depth increases almost linearly with spacing ratio. This suggests that if plugging is required, selection of spacing ratio will depend on the allowable settlement of the structure. In Fig. 11(b) the plugging penetration is normalised by foundation breadth B, and in Fig. 11(c) by the space between adjacent grilles ($s-t$), which might be expected to control the amount of plugging. The solutions converge with increasing s/t for $z_{\mathrm{plug}}/(s-t)$, suggesting that this might be the most appropriate normalisation.

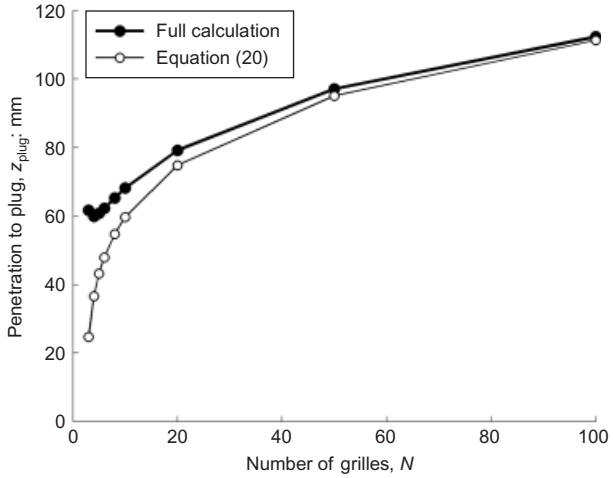

Fig. 10. Calculated plugging penetration against number of grilles (loose sand; $s/t = 4$)

Given that a typical maximum grille height is ≈50 mm, this represents an upper limit on the allowable settlement of the foundation. From Fig. 11(a) it will be seen that, for $N = 5$, only grillages with $s/t < 3{\cdot}5$ are expected to achieve the fully plugged capacity for less than 50 mm penetration (using the full calculation results). This would suggest that in the experiments with $N = 5$ (Table 2), only test V16 would be expected to plug ($s/t = 2{\cdot}5$), and that this is expected to occur at $z \approx 25$ mm.

In order to observe the onset of plugging, the sequence of images taken during the vertical load tests was analysed using GeoPIV (White *et al.*, 2003). Fig. 12 shows incremental soil displacements at various penetration depths for test V16 ($s/t = 2{\cdot}5$). The images in which the displacement vectors are plotted are those at the start of the increment (i.e. the initial position of the soil for that increment). It will be seen that early in the test (Fig. 12(a)) the grillage is coring, as there is evidence of slight heave of soil between the grilles between the first pair of images ($z = 0$–6 mm). Similar behaviour was observed up until the increment $z = 18$–24 mm. In Fig. 12(b) the image (taken at $z = 18$ mm) shows that the soil between the grilles is essentially at the same level as that outside the grilles (although there is some surface distortion close to the grilles), suggesting that plugging has not yet started. However, the displacement vectors for this increment show the soil between the grilles moving uniformly downwards with the grillage, indicating the onset of plugging. This plugged behaviour continued until the end of the test. Fig. 12(c) shows the displacement increment around 50 mm penetration. The soil between the grilles has plugged and displaced significantly downwards compared with the soil outside the grillage (note that, because of the difference in level, some

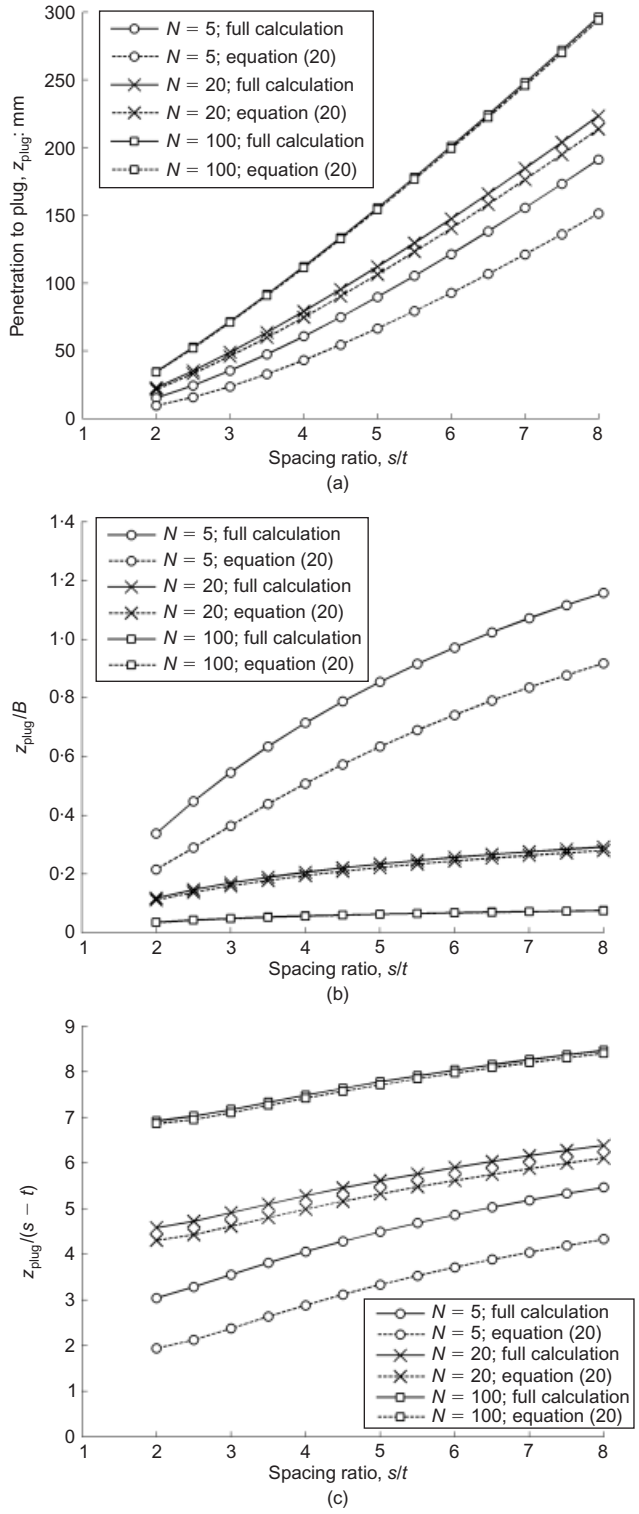

Fig. 11. Predicted plugging depths for loose sand ($K = 0{\cdot}75$, $\delta = 21{\cdot}7°$, $\phi = 30{\cdot}8°$): (a) not normalised; (b) normalised by B; (c) normalised by $s - t$

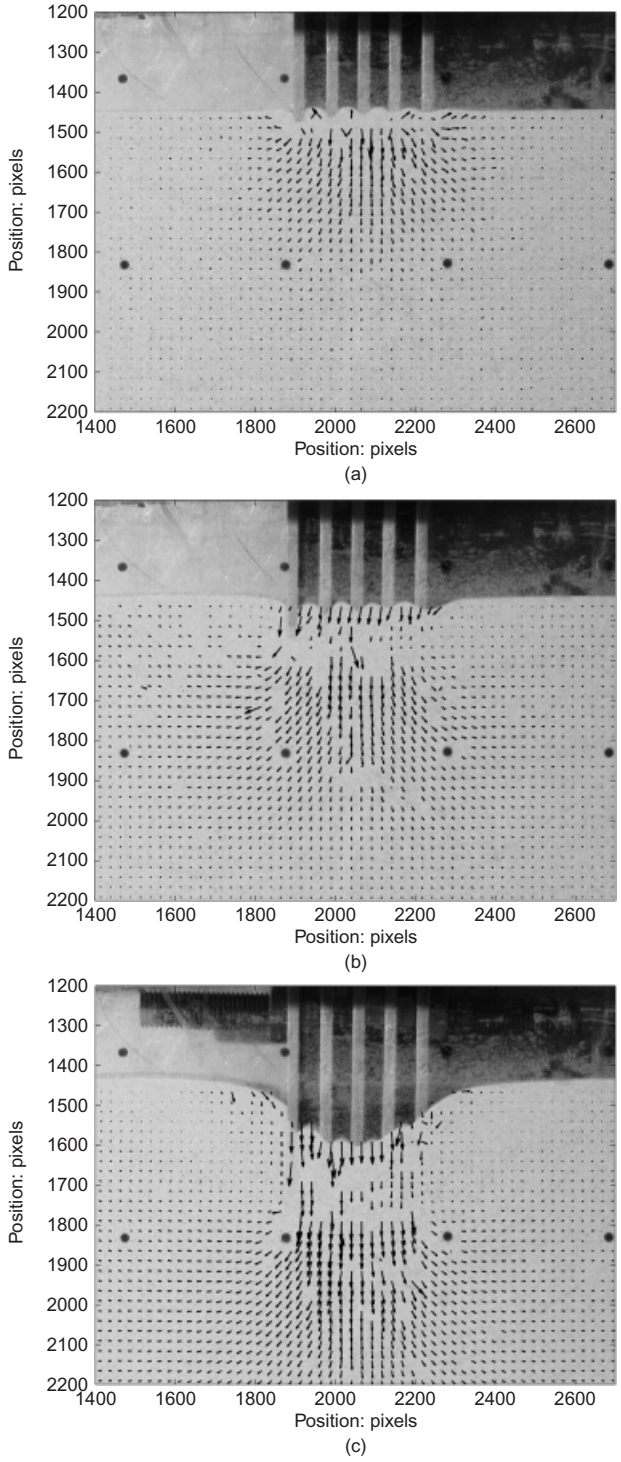

Fig. 12. Incremental soil displacements observed in test V16 ($s/t = 2{\cdot}5$): (a) increment $z = 0$–6 mm; (b) increment $z = 18$–24 mm (onset of plugging); (c) increment $z = 47$–53 mm (maximum allowable penetration)

soil has fallen in between the grille and the Perspex). These observations would suggest that in the experiment the grillage plugged at $18 < z_{plug} < 24$ mm. This compares favourably with the value of 25 mm predicted from the analytical solution (Fig. 11(a)), and is consistent with the change in the gradient of the load–penetration curve at $z \approx 20$ mm (Fig. 5(a)).

Figure 13 shows PIV observations from tests V18 and V11 (i.e. $s/t = 6$ and 8 respectively). Only data for the last displacement increment ($z \approx 50$ mm) are plotted, as in both cases plugging was not observed, even at this penetration. This is in agreement with the analytical solution, which does not predict plugging for $z \leqslant 50$ mm. Because of a malfunction with the digital camera, no images were available for test V5 ($s/t = 4$). Nonetheless, the experimental data appear to support the results of the analytical model, at least in loose sand.

Figure 14 shows the predicted vertical capacity of the foundation in terms of the fully plugged capacity as a function of spacing ratio for different amounts of penetration using the full calculation method. Fig. 14(a) has been plotted

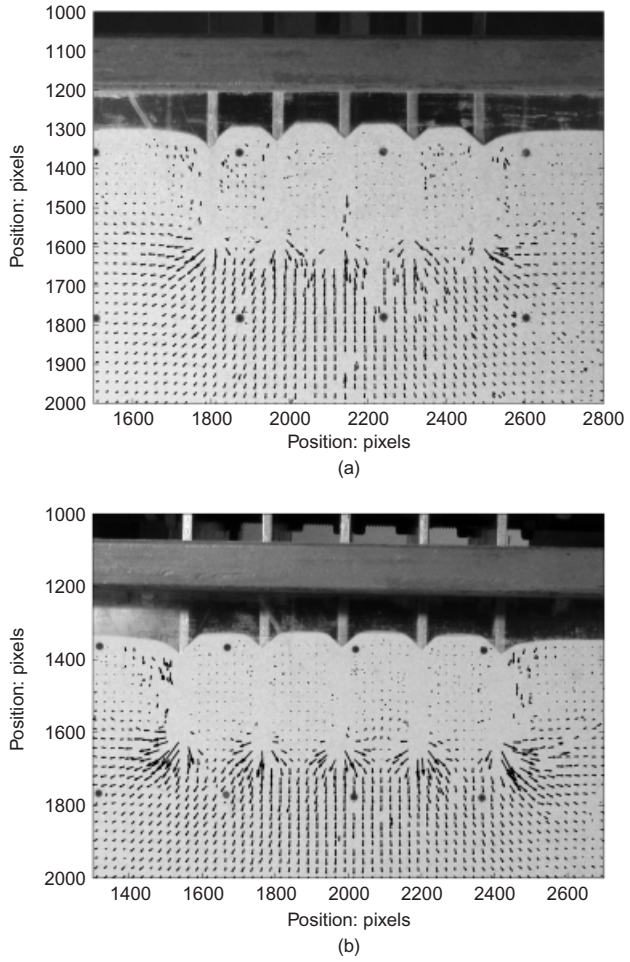

Fig. 13. Observed incremental soil displacements at full penetration of grillage ($z \approx 50$ mm): (a) test V18 ($s/t = 6$), increment $z = 47$–53 mm; (b) test V11 ($s/t = 8$), increment $z = 49$–55 mm

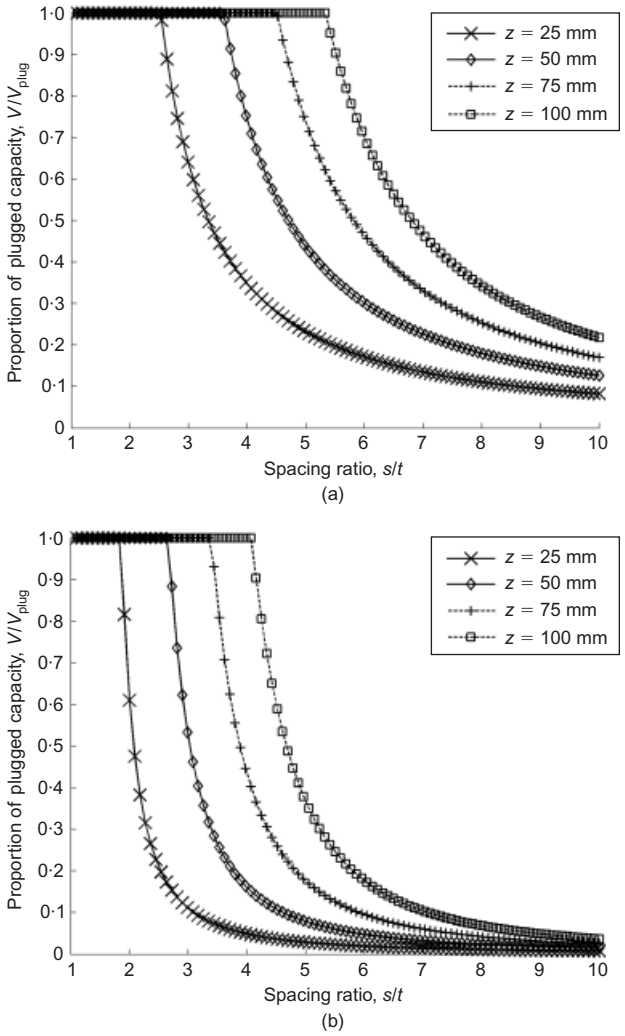

Fig. 14. Grillage capacity and onset of plugging as a function of s/t for different penetration depths (loose sand): (a) experimental conditions ($N = 5$); (b) full-size grillage ($N = 50$)

for the experimental conditions ($N = 5$), which confirms that plugging is expected at $z = 25$ mm for $s/t = 2{\cdot}5$, that test V5 ($s/t = 4$) may have started to plug at the very limit of the allowable penetration (had images been available to verify this), and that for $s/t = 6$ and 8 plugging was not expected to occur. Fig. 14(b) shows a similar plot for $N = 50$, closer to that expected for a full-size grillage. It will be seen that spacing ratio is more critical at higher N if the fully plugged capacity needs to be reached.

Prediction of penetration for equivalent flat-plate capacity

The capacity of conventional flat (i.e. not grilled) mudmat foundations is likely to be calculated with equation (1), assuming no embedment. This is a conservative solution, because a foundation will work-harden with increased penetration. This calculated value of V will be used (together with their sliding capacity) to ensure flat foundation sizes are appropriate. Consequently, it may be informative to find the amount of penetration that a grillage foundation requires to mobilise this design bearing capacity.

As before, this was accomplished both numerically by increasing the penetration until the pile solution equalled the flat plate ($z = 0$) capacity, and by simplifying the equations to give an analytical solution. The same assumptions were made as for the plug depth calculations in the previous section. Equation (19) then becomes simpler, because there is no depth term in the flat-plate bearing capacity equation. When the grillage capacity equals the flat-plate capacity

$$N\sigma'_{\mathrm{v}} t N_{q\mathrm{B}} = 0{\cdot}5 N_\gamma \gamma' B^2 \tag{21}$$

When equation (12) is substituted, the penetration depth for equivalent flat plate capacity, z_0, can be expressed as

$$z_0 = \frac{\ln\left[1 + 0{\cdot}5aB\left(\frac{B}{Nt}\right)\left(\frac{N_\gamma}{N_{q\mathrm{B}}}\right)\right]}{a} \tag{22}$$

For large values of N, B may be approximated as Ns. If this is substituted along with a, then

$$z_o = \frac{\ln\left[1 + K\tan\delta'\left(\frac{B}{s-t}\right)\left(\frac{s}{t}\right)\left(\frac{N_\gamma}{N_{qB}}\right)\right]}{2K\tan\delta'}(s-t) \tag{23}$$

The form of equation (23) would seem to confirm that $z_0/(s-t)$ is the most appropriate normalisation for the plugging depth, as shown in Fig. 11(c).

Figure 15 shows the calculated penetration depth z_0 required to reach the calculated flat-plate capacity for different breadth foundations with spacing $s/t = 4$, $t = 5$ mm in loose sand. There is good agreement between equation (23) and the full calculation method, confirming that the simplified equation may be suitably accurate. The analytical results suggest that large foundations will require displacements of approximately 70 mm to reach the equivalent flat-plate capa-

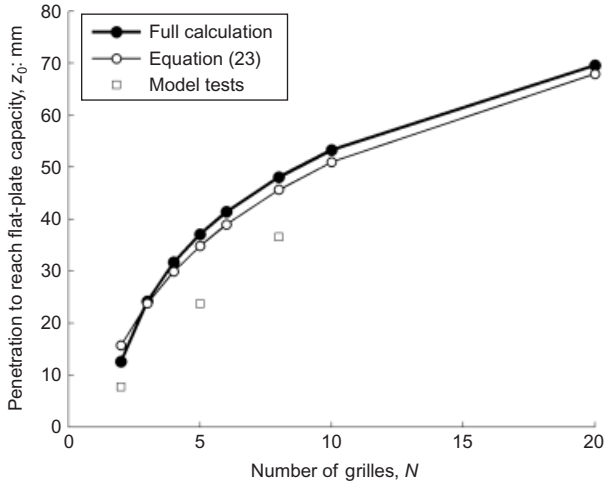

Fig. 15. Calculated penetration to reach flat-plate capacity ($s/t = 4$; loose sand)

city. The test data points are also shown in Fig. 15, and show that the analytical solution given by equation (23) provides a conservative estimate (overprediction) of the amount of penetration required to achieve the equivalent flat-plate capacity $V_{0,\text{flatplate}}$.

Figure 16 shows the calculated foundation penetrations required to generate the flat-plate capacity for a range of spacing ratios. As before, the displacements are shown without normalisation (Fig. 16(a)), normalised by B (Fig. 16(b)), and normalised by $s - t$ (Fig. 16(c)). As the spacing ratio s/t increases, the required displacement, $z_0/(s - t)$, increases gradually because of the logarithmic term in equations (22) and (23).

Figure 17 shows the grillage capacity normalised by the equivalent flat-plate capacity as a function of spacing ratio for the maximum allowable penetration ($z = 50$ mm), both as predicted and as observed in the model tests. This line represents the maximum allowable capacity as a function of s/t. The actual proportion of $V_{0,\text{flatplate}}$ mobilised by the end of each test is in all cases larger than the predictions from the analytical model, suggesting that the analytical model is conservative, at least in loose sand. The predictions for $N = 2$ do not match the model test data as closely as those for $N = 5$ and 8, which may be attributed to the end effects on the outside grilles described previously, which are not negligible when only two grilles are present. Generally, the analytical model gives more accurate predictions as N is increased, as the outside grilles contribute less to the total grillage capacity. This suggests that the model is suitable for use in the design of full-size foundations where $N \approx 10^2$.

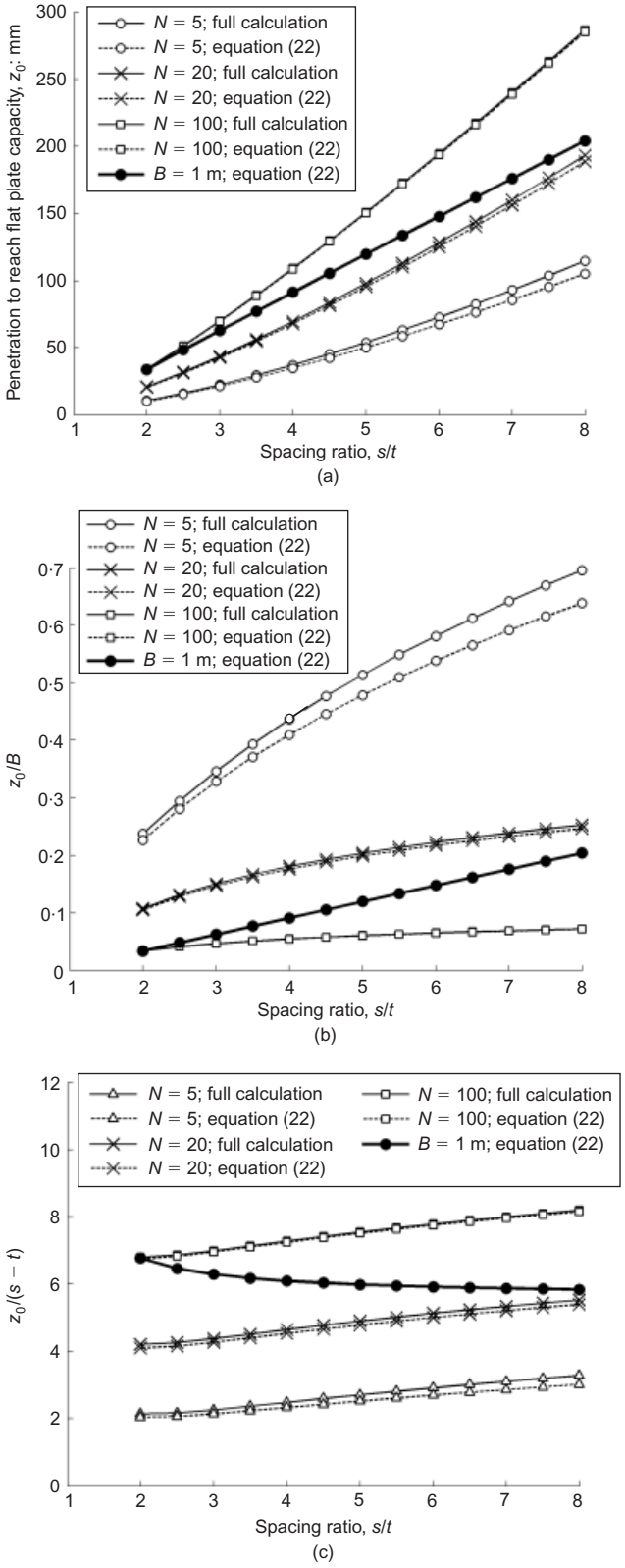

Fig. 16. Foundation penetration required to generate flat-plate capacity ($V_{0,\text{flatplate}}$): (a) not normalised; (b) normalised by foundation breadth; (c) normalised by $s - t$

CONCLUSIONS

A new analytical method has been developed to calculate the bearing capacity of grillage foundations in drained cohesionless soil. This method has been used to investigate the likely characteristics of grillage foundation capacity in terms of the load–displacement characteristics and soil deformation mechanisms.

Additional simplified analytical equations were produced for predicting penetration depth under a given load (equation (18)), the depth of penetration required to generate the capacity of an equivalent flat plate foundation with no settlement (equations (22) and (23)), and the foundation penetration required to plug the grilles fully (equation (20)). These simplified equations were compared with results from the full analysis, with good agreement.

Analytical results were validated with a series of physical model tests conducted in loose sand conditions. Good agreement was obtained between load–displacement behaviour, the onset of plugging and observed soil-displacement mechanisms. Loose sand conditions were investigated, as this was believed to be the most onerous ground condition for grillage design. Future work should validate the new analytical methodology for soils with different densities. Grillage

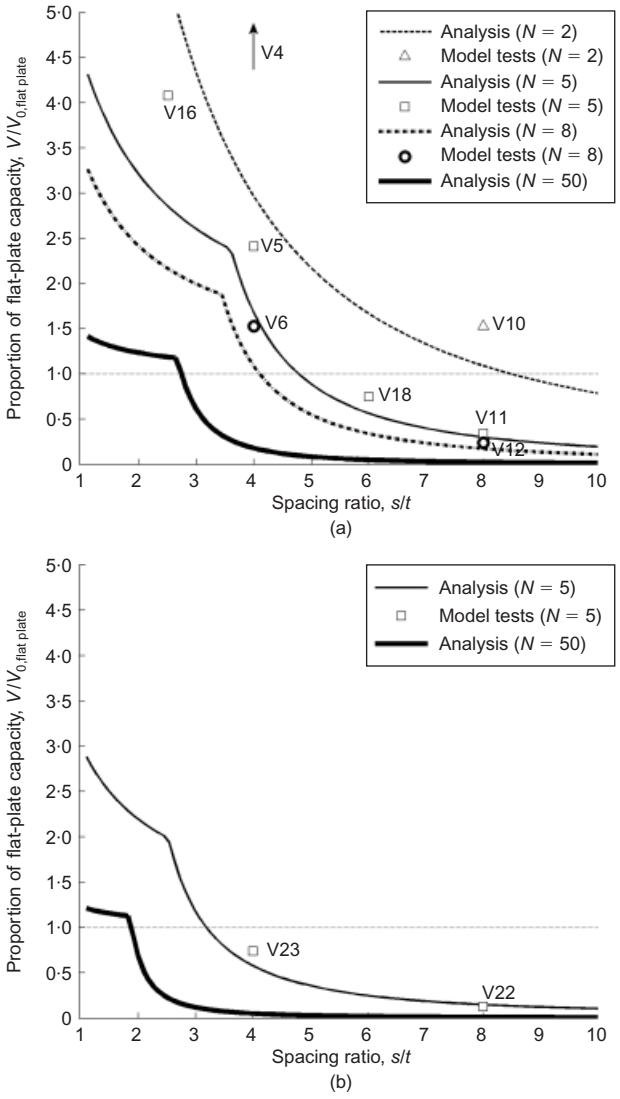

Fig. 17. Bearing capacity of grillage foundations for $z = 50$ mm, loose sand: (a) $t = 5$ mm; (b) $t = 10$ mm

foundations appear to be capable of providing sufficient vertical bearing capacity to replace conventional mudmats of equivalent breadths, even in loose sand conditions, albeit at the expense of vertical settlement.

ACKNOWLEDGEMENTS

The experimental work was carried out as part of a joint industry project funded by Acergy, Subsea 7 and Technip. The project was managed by Cathie Associates. The authors are grateful for technical discussion of the project findings by Neil Brown, David Cathie, Ronye Egborge, Alasdair Maconochie, Neil Morgan, Andrew Ripley and GiJae Yun.

NOTATION

A foundation base area
A_b base area of grille
a $2K\tan\delta'/(s-t)$
B foundation breadth
c' apparent cohesion
D grille height
D_r relative density
d_q, d_γ depth correction factors
d_{10} particle size below which 10% of particles are smaller
d_{50} mean particle size
K coefficient of lateral earth pressure
K_0 coefficient of lateral earth pressure at rest
L foundation/grille length
N number of grilles
N_q bearing capacity factor (overburden)
N_{qB} bearing capacity factor (grille base)
N_γ bearing capacity factor (self-weight)
Q_b base capacity of grille
Q_{bi} base resistance of each grille in inside of group
Q_{bo} base resistance of each of two external (edge) grilles
Q_s skin friction
Q_{si} skin friction on one side of each internal grille
Q_{so} skin friction on outside grille surfaces
q foundation bearing pressure
q_f bearing pressure at failure
s grille spacing
t grille thickness
V vertical load/pure vertical load capacity
V_{plug} vertical load for full plugging between grilles
$V_{0,flatplate}$ vertical load capacity for flat-plate foundation (at $z = 0$)
W self-weight vertical load
z grille penetration
z_{plug} grille penetration required to plug
z_0 grille penetration to obtain equivalent flat-plate capacity (at $z = 0$)
γ' effective unit weight of soil
δ' angle of interface friction
ρ soil density
ρ_{max} maximum soil density
ρ_{min} minimum soil density
σ'_v vertical effective stress
σ'_{vb} vertical effective stress at level of grille tips
τ skin friction at the grille–sand interface
ϕ' angle of internal friction of soil
ϕ'_{peak} peak angle of internal friction of soil

REFERENCES

Berezantzev, V. G., Khristoforov, V. S. & Golubkov, V. N. (1961). Load bearing capacity and deformation of piled foundations. *Proc. 5th Int. Conf. Soil Mech. Found. Engng, Paris*, 11–15.

BSI (1990). *Methods of test for soils for civil engineering purposes: General requirements and sample preparation*, BS1377-1. Milton Keynes: British Standards Institution.

DNV (1992). *Classification notes No. 30·4; Foundations*. Oslo: Det Norske Veritas.

Fisher, R. & Cathie, D. (2003). Optimisation of gravity based design for subsea applications. *Proceedings of the BGA international conference on foundations*, Dundee, pp. 283–296.

Graham, J., Raymond, G. P. & Suppiaha, A. (1984). Bearing capacity of three closely-spaced footings on sand. *Géotechnique* **34**, No. 2, 173–182, http://dx.doi.org/10.1680/geot.1984.34.2.173.

Hansen, J. B. (1970). A revised and extended formula for bearing capacity. *Bull. Danish Geotech. Inst.*, No. 28, 5–11.

Jaky, J. (1944). The coefficient of earth pressure at rest. *J. Soc. Hungarian Arch. Engrs* **78**, No. 22, 355–358.

Javadi, A. & Spoor, G. (2004). Soil failure patterns and load–sinkage relationships under interacting shallow footing and wheel arrangements. *Biosyst. Engng* **88**, No. 3, 383–393.

Kulhawy, F. H. (1984). Limiting tip and side resistance, fact or fallacy. *Proceedings of the symposium on analysis and design of piled foundations*, San Francisco, pp. 80–98.

Kumar, J. & Ghosh, P. (2007). Ultimate bearing capacity of two interfering rough strip footings. *Int. J. Geomech.* **7**, No. 1, 53–62.

Randolph, M. F., Leong, E. C. & Houlsby, G. T. (1991). One-dimensional analysis of soil plugs in pipe piles. *Géotechnique* **41**, No. 4, 587–598, http://dx.doi.org/10.1680/geot.1991.41.4.587.

Reissner, H. (1924). Zum Erddruckproblem. *Proc. 1st Int. Conf. Appl. Mech., Delft*, 295–311.

Stuart, J. G. (1962). Interference between foundations, with special reference to surface footings in sand. *Géotechnique* **12**, No. 1, 15–22, http://dx.doi.org/10.1680/geot.1962.12.1.15.

White, D. J., Take, W. A. & Bolton, M. D. (2003). Soil deformation measurement using particle image velocimetry and photogrammetry. *Géotechnique* **53**, No. 7, 619–631, http://dx.doi.org/10.1680/geot.2003.53.7.619.